Journal of Contaminant Hydrology 120–121 (2011) 18–26

Contents lists available at ScienceDirect

Journal of Contaminant Hydrology

journal homepage: www.elsevier.com/locate/jconhyd

Applicability regimes for macroscopic models of reactive transport in porous media

I. Battiato, D.M. Tartakovsky *

Department of Mechanical and Aerospace Engineering, University of California, San Diego, La Jolla, CA 92093, USA

ARTICLE INFO

Available online 26 May 2010

Keywords:
Upscaling
Homogenization
Homogeneous reaction
Heterogeneous reaction
Dissolution
Precipitation
Multiple scale expansion

ABSTRACT

We consider transport of a solute that undergoes a nonlinear heterogeneous reaction: after reaching a threshold concentration value, it precipitates on the solid matrix to form a crystalline solid. The relative importance of three key pore-scale transport mechanisms (advection, molecular diffusion, and reaction) is quantified by the Péclet (Pe) and Damköhler (Da) numbers. We use multiple-scale expansions to upscale a pore-scale advection–diffusion equation with reactions entering through a boundary condition on the fluid–solid interface, and to establish sufficient conditions under which macroscopic advection–dispersion-reaction equations provide an accurate description of the pore-scale processes. These conditions are summarized by a phase diagram in the (Pe, Da)-space, parameterized with a scale-separation parameter that is defined as the ratio of characteristic lengths associated with the pore- and macro-scales.

1. Introduction

Nonlinear reactive transport in porous media can be described with either pore-scale or Darcy-scale (macroscopic) models. Pore-scale simulations have a solid physical foundation, but require the knowledge of pore geometry that is seldom available and are impractical as a predictive tool at scales that are orders of magnitude larger than the pore scale. Macroscopic (effective, upscaled, continuum, homogenized, etc.) models, which represent a porous medium as an averaged continuum, overcome these limitations at the cost of relying on largely phenomenological descriptions and/or closure assumptions. While useful in a variety of applications, upscaled models often fail to capture a number of experimentally observed transport features, including asymmetrical long tails of breakthrough curves (Neuman and Tartakovsky, 2009), the extent of reactions in mixing-controlled chemical transformations (Knutson et al., 2007; Li et al., 2006), the onset of instability in variable density flows and the disparity in fractal dimensions of diffusion and dispersion fronts (Maloy et al., 1998).

These shortcomings manifest themselves when approximations and/or closure assumptions underlying continuum models are violated. Regardless of which upscaling approach is used—e.g., volume averaging, the method of moments, pore-network models, homogenization via multiple-scale expansions and its modifications, and thermodynamically constrained averaging (see (Battiato et al., 2009) for references)—nonlinearities of pore-scale governing equations and/or boundary conditions require linearization and other approximations that may render macroscopic representations of pore-sale processes inadequate.

Most upscaling studies focus on the derivation of effective models that relate microscopic (pore-scale) characteristics of a porous medium and/or fluid processes to their macroscopic (continuum, meso- or Darcy-scale) counterparts (Hesse et al., 2009, and the references therein). In doing so, one disregards certain terms in an averaging (homogenization) procedure by claiming, for example, that fluctuations about their respective means are small and can be neglected. Such approaches establish connections between physicochemical processes on different scales, provided the underlying assumptions hold. However, they cannot be used to identify the validity of these assumptions and the regions of a computational domain wherein a continuum (effective) model breaks down. The

* Corresponding author. Tel.: +1 858 534 1375.
E-mail address: dmt@ucsd.edu (D.M. Tartakovsky).

0169-7722/$ – see front matter © 2010 Elsevier B.V. All rights reserved.
doi:10.1016/j.jconhyd.2010.05.005

latter is essential for hybrid simulations, which employ pore-scale and continuum descriptions of the same phenomenon in different regions of a computational domain (Tartakovsky et al., 2008).

Upscaling approaches that rely on characteristic dimensionless numbers (e.g., the Damköhler and Péclet numbers) can provide quantitative measures for the validity of various upscaling approximations. For example, the Péclet number (Pe) determines whether an advection–dispersion equation provides an effective representation of pore-scale dispersion (Auriault and Adler, 1995); the Damköhler number (Da) can be used to predict the breakdown of continuum models of simultaneous pore-scale diffusion and nonlinear homogeneous and linear heterogeneous reactions (Battiato et al., 2009); and both Da and Pe determine whether transport in a capillary tube due to advection, diffusion and linear heterogeneous reactions is homogenizable (Mikelic et al., 2006).

We investigate the conditions under which continuum descriptions of reactive transport, i.e., advection–dispersion-reaction equations (ARDEs), break down. In Section 2, we formulate a pore-scale model of nonlinear crystal dissolution–precipitation, and identify the Damköhler and Péclet numbers as dimensionless parameters that control the phenomenon. In Section 3, we employ a multiple-scale expansion (Auriault and Adler, 1995; Hornung, 1997) to derive an effective ARDE and to specify sufficient conditions that guarantee its validity. The region of validity of this continuum description is represented by a phase diagram in the (Da, Pe)-space. A number of special cases are discussed in Section 4. The main results and conclusions are summarized in Section 5.

2. Problem formulation

Consider reactive transport in a porous medium $\hat{\Omega}$ whose characteristic length is L. Let us assume that the medium can be represented microscopically by a collection of spatially periodic "unit cells" $\hat{Y}$ with a characteristic length ℓ, such that a scale parameter $\varepsilon \equiv \ell/L \ll 1$. Spatially periodic representations of micro-structures of porous media are routinely used to derive macroscopic properties and effective models of phenomena taking place in disordered media that lack such periodicity (Nitsche and Brenner, 1989, Section 2). The unit cell $\hat{Y} = \hat{\mathcal{B}} \cup \hat{\mathcal{G}}$ consists of the pore-space $\hat{\mathcal{B}}$ and the impermeable solid matrix $\hat{\mathcal{G}}$ that are separated by the smooth surface $\hat{\Gamma}$. The pore-spaces $\hat{\mathcal{B}}$ of each cell $\hat{Y}$ form the multi-connected pore-space domain $\hat{\mathcal{B}}^\varepsilon \subset \hat{\Omega}$ bounded by the smooth surface $\hat{\Gamma}^\varepsilon$.

2.1. Governing equations

Single-phase flow of an incompressible fluid in the pore-space $\hat{\mathcal{B}}^\varepsilon$ is described by the Stokes and continuity equations subject to the no-slip boundary condition on $\hat{\Gamma}^\varepsilon$,

$$\hat{\nu}\,\hat{\nabla}^2 \hat{\mathbf{v}}_\varepsilon - \hat{\nabla}\hat{p} = 0, \quad \hat{\nabla}\cdot\hat{\mathbf{v}}_\varepsilon = 0, \quad \hat{\mathbf{x}} \in \hat{\mathcal{B}}^\varepsilon, \qquad \hat{\mathbf{v}}_\varepsilon = 0, \quad \hat{\mathbf{x}} \in \hat{\Gamma}^\varepsilon, \tag{1}$$

where $\hat{\mathbf{v}}_\varepsilon(\hat{\mathbf{x}})$ is the fluid velocity, $\hat{p}$ denotes the fluid dynamic pressure, and $\hat{\nu}$ is the dynamic viscosity. The fluid contains a dissolved species $\mathcal{M}$, whose molar concentration $\hat{c}_\varepsilon(\hat{\mathbf{x}},\hat{t})$ $[molL^{-3}]$ at point $\hat{\mathbf{x}} \in \hat{\mathcal{B}}^\varepsilon$ and time $\hat{t} > 0$ changes due to advection, molecular diffusion, and a nonlinear heterogeneous reaction at the solid–liquid interface $\hat{\Gamma}^\varepsilon$. The first two phenomena are described by an advection–diffusion equation,

$$\frac{\partial \hat{c}_\varepsilon}{\partial \hat{t}} + \hat{\mathbf{v}}_\varepsilon \cdot \hat{\nabla}\,\hat{c}_\varepsilon = \hat{\nabla}\cdot\left(\hat{\mathbf{D}}\hat{\nabla}\hat{c}_\varepsilon\right), \qquad \hat{\mathbf{x}} \in \hat{\mathcal{B}}^\varepsilon, \quad \hat{t} > 0, \tag{2}$$

where the molecular diffusion coefficient $\hat{D}$ is, in general, a positive-definite second-rank tensor. If diffusion is isotropic, $\hat{D} = \hat{\mathcal{D}}_m \mathbf{I}$ where $\hat{\mathcal{D}}_m$ $[L^2T^{-1}]$ is the diffusion coefficient and $\mathbf{I}$ is the identity matrix.

Whenever the concentration $\hat{c}_\varepsilon$ exceeds a threshold value $\bar{c}$, a heterogeneous reaction $n\mathcal{M} \leftrightarrow \mathcal{N}_{(s)}$ occurs, in which n molecules of the solute $\mathcal{M}$ precipitate in the form of one molecule of a crystalline solid $\mathcal{N}_{(s)}$. At the solid–liquid interface $\hat{\Gamma}^\varepsilon$ impermeable to flow, mass conservation requires that mass flux of the species $\mathcal{M}$ be balanced by the difference between the precipitation rate R_p and the dissolution rate R_d,

$$-\mathbf{n}\cdot\hat{\mathbf{D}}\hat{\nabla}\hat{c}_\varepsilon = R_p - R_d, \tag{3}$$

where $\mathbf{n}$ is the outward unit normal vector of $\hat{\Gamma}^\varepsilon$. Following (Knabner et al., 1995), we assume that $R_p = \hat{k}\hat{c}_\varepsilon^a$ and $R_d = \hat{k}\bar{c}^a$, where $\hat{k}$ $[L^{3a-2}T^{-1}mol^{1-a}]$ is the reaction rate constant, $a \in \mathbb{Z}^+$ is related to the order of reaction n (Morse and Arvidson, 2002, Eq. 6), and the threshold concentration $\bar{c}$ represents the solubility product (Morse and Arvidson, 2002). Mass conservation on the liquid–solid interface $\hat{\Gamma}^\varepsilon$ yields a boundary condition (Morse and Arvidson, 2002, Eq. 5),

$$-\mathbf{n}\cdot\hat{\mathbf{D}}\hat{\nabla}\hat{c}_\varepsilon = \hat{k}\left(\hat{c}_\varepsilon^a - \bar{c}^a\right), \qquad \hat{\mathbf{x}} \in \hat{\Gamma}^\varepsilon, \quad \hat{t} > 0. \tag{4}$$

In addition to Eq. (4), the flow and transport Eqs. (1) and (2) are supplemented with proper boundary conditions on the external boundary of the flow domain $\hat{\Omega}$.

2.2. Dimensionless formulation

Let us introduce dimensionless quantities

$$c_\varepsilon = \frac{\hat{c}_\varepsilon}{\bar{c}}, \quad \mathbf{x} = \frac{\hat{\mathbf{x}}}{L}, \quad \mathbf{v}_\varepsilon = \frac{\hat{\mathbf{v}}_\varepsilon}{U}, \quad \mathbf{D} = \frac{\hat{\mathbf{D}}}{D}, \quad p = \frac{\hat{p}\ell^2}{\hat{\nu}UL}, \tag{5}$$

where D and U are characteristic values of $\hat{\mathbf{D}}$ and $\hat{\mathbf{v}}_\varepsilon$, respectively. The scaling of pressure $\hat{p}$ ensures that the pressure gradient and the viscous term are of the same order of magnitude, as prescribed by the Stokes equations (Auriault and Adler, 1995, Eqs. 15 and 16). Furthermore, we define three time scales associated with diffusion ($\hat{t}_D$), reactions ($\hat{t}_R$) and advection ($\hat{t}_A$) as

$$\hat{t}_D = \frac{L^2}{D}, \quad \hat{t}_R = \frac{L}{\hat{k}\bar{c}^{a-1}}, \quad \hat{t}_A = \frac{L}{U}. \tag{6}$$

Ratios between these time scales define the dimensionless Damköhler ($\mathrm{Da} = \hat{t}_D/\hat{t}_R$) and Péclet ($\mathrm{Pe} = \hat{t}_D/\hat{t}_A$) numbers,

$$\mathrm{Da} = \frac{L\hat{k}\bar{c}^{a-1}}{D} \quad \text{and} \quad \mathrm{Pe} = \frac{UL}{D}. \tag{7}$$

Rewriting Eqs. (1)–(4) in terms of the dimensionless quantities (5) and the dimensionless time $t=\hat{t}/\hat{t}_D$ yields a dimensionless form of the flow equations

$$\varepsilon^2\nabla^2\mathbf{v}_\varepsilon-\nabla p=0,\qquad \nabla\cdot\mathbf{v}_\varepsilon=0,\qquad \mathbf{x}\in\mathcal{B}^\varepsilon, \tag{8}$$

subject to

$$\mathbf{v}_\varepsilon=0,\qquad \mathbf{x}\in\Gamma^\varepsilon, \tag{9}$$

and a dimensionless form of the transport equation

$$\frac{\partial c_\varepsilon}{\partial t}+\nabla\cdot(-\mathbf{D}\nabla c_\varepsilon+\mathrm{Pe}\mathbf{v}_\varepsilon c_\varepsilon)=0,\qquad \mathbf{x}\in\mathcal{B}^\varepsilon,\qquad t>0, \tag{10}$$

subject to

$$-\mathbf{n}\cdot\mathbf{D}\nabla c_\varepsilon=\mathrm{Da}(c_\varepsilon^a-1),\qquad \mathbf{x}\in\Gamma^\varepsilon,\qquad t>0. \tag{11}$$

2.3. Periodic geometry and periodic coefficients

The boundary-value problems (8)–(9) and (10)–(11) are defined for the pore-space $\mathcal{B}^\varepsilon$ composed of periodically repeating unit cells $\mathcal{B}$. These problems have constant coefficients (the fluid viscosity ν and the molecular diffusion coefficient $\mathbf{D}$) but have to be solved in the highly irregular flow domain $\mathcal{B}^\varepsilon$. Alternatively, one can define these problems on a regular domain, the porous medium Ω composed of both the solid matrix $\mathcal{G}$ and the pore space $\mathcal{B}$, by introducing spatially varying coefficients. This is accomplished as follows (see (Hornung, 1997) for more details).

Let us introduce a scaled membership function $\pi_\varepsilon(\mathbf{x})=\pi_\varepsilon(\mathbf{x}/\varepsilon)$, where $\pi_\varepsilon(\mathbf{x})$ is an indicator (membership) function

$$\pi(\mathbf{x})=\begin{cases}1, & \mathbf{x}\in\mathcal{B}\\ 0, & \mathbf{x}\in\mathcal{G}.\end{cases} \tag{12}$$

Then one can define spatially varying coefficients everywhere in the domain Ω,

$$\mathbf{D}_\varepsilon(\mathbf{x})\equiv\pi_\varepsilon(\mathbf{x})\mathbf{D},\qquad \nu_\varepsilon(\mathbf{x})\equiv\pi_\varepsilon(\mathbf{x})\nu,\qquad \mathbf{x}\in\Omega. \tag{13}$$

By construction, the functions $\mathbf{D}_\varepsilon(\mathbf{x})$ and $\nu_\varepsilon(\mathbf{x})$ are periodic with the period Y determined by the unit cell size. Eqs. (8) and (10) can now be defined on the domain Ω,

$$\varepsilon^2\nu_\varepsilon\nabla^2\tilde{\mathbf{v}}_\varepsilon-\nabla\tilde{p}_\varepsilon=0,\quad \frac{\partial\tilde{c}_\varepsilon}{\partial t}+\nabla\cdot(-\mathbf{D}_\varepsilon\nabla\tilde{c}_\varepsilon+\mathrm{Pe}\tilde{\mathbf{v}}_\varepsilon\tilde{c}_\varepsilon)=0,\quad \mathbf{x}\in\Omega, \tag{14}$$

where the state variables $(\tilde{\mathbf{v}}_\varepsilon,\tilde{p}_\varepsilon,\tilde{c}_\varepsilon)$ are respective extensions to Ω of their counterparts $(\mathbf{v}_\varepsilon, p_\varepsilon, c_\varepsilon)$. The two sets of these state variables coincide in $\mathcal{B}^\varepsilon$ (Hornung, 1997, pp.14,15, and 46).

3. Homogenization via multiple-scale expansions

Homogenization aims to derive effective equations for averaged state variables that are representative of an averaging volume (e.g., Darcy-scale). To this end, three types of local averages of a quantity $\mathcal{A}(\mathbf{x})$ can be defined,

$$\langle\mathcal{A}\rangle\equiv\frac{1}{|Y|}\int_{\mathcal{B}(\mathbf{x})}\mathcal{A}\mathrm{d}\mathbf{y},\quad \langle\mathcal{A}\rangle_{\mathcal{B}}\equiv\frac{1}{|\mathcal{B}|}\int_{\mathcal{B}(\mathbf{x})}\mathcal{A}\mathrm{d}\mathbf{y},\quad \langle\mathcal{A}\rangle_{\Gamma}\equiv\frac{1}{|\Gamma|}\int_{\Gamma(\mathbf{x})}\mathcal{A}\mathrm{d}\mathbf{y}, \tag{15}$$

where $\langle\mathcal{A}\rangle=\phi\langle\mathcal{A}\rangle_{\mathcal{B}}$ and $\phi=|\mathcal{B}|/|Y|$ is the porosity. In the subsequent derivation of effective (continuum- or Darcy-scale) equations for average flow velocity $\langle\mathbf{v}(\mathbf{x})\rangle$ and solute concentration $\langle c(\mathbf{x},t)\rangle$, we employ the method of multiple-scale expansions (Auriault and Adler, 1995; Hornung, 1997).

3.1. Upscaled flow equations

Upscaling of the Stokes Eqs. (8) and (9) at the pore-scale to the continuum scale has been the subject of numerous investigations, including those relying on multiple-scale expansions (Auriault and Adler, 1995; Hornung, 1997; Mikelic et al., 2006). These studies have demonstrated that Darcy's law and the continuity equation for $\langle\mathbf{v}\rangle$,

$$\langle\mathbf{v}\rangle=-\mathbf{K}\cdot\nabla p_0,\qquad \nabla\cdot\langle\mathbf{v}\rangle=0,\qquad \mathbf{x}\in\Omega, \tag{16}$$

provide an effective representation of the pore-scale Stokes flow (e.g., Hornung, 1997, Eq. 4.7). Such homogenization procedures also enable one to formally define the dimensionless permeability tensor $\mathbf{K}$ in Eq. (16) as the average, $\mathbf{K}=\langle\mathbf{k}(\mathbf{y})\rangle$, of a "closure variable" $\mathbf{k}(\mathbf{y})$. The latter is the unique solution of a local, or unit cell, problem (e.g., Hornung, 1997, pp. 46–47, Theorem 1.1; and Auriault and Adler, 1995, Eq. 22)

$$\nabla^2\mathbf{k}+\mathbf{I}-\nabla\mathbf{a}=\mathbf{0},\qquad \nabla\cdot\mathbf{k}=\mathbf{0},\qquad \mathbf{y}\in\mathcal{B} \tag{17}$$

subject to the boundary condition $\mathbf{k}(\mathbf{y})=\mathbf{0}$ for $\mathbf{y}\in\Gamma$. The vector $\mathbf{a}$ is Y-periodic and satisfies the condition $\langle\mathbf{a}\rangle=\mathbf{0}$. Consequently, the second-order tensor $\mathbf{k}$ is Y-periodic as well.

3.2. Upscaled transport equation

The method of multiple-scale expansions introduces a fast space variable $\mathbf{y}$ and two time variables τ_r and τ_a,

$$\mathbf{y}=\frac{\mathbf{x}}{\varepsilon},\qquad \tau_r=t\mathrm{Da}=\frac{\hat{t}}{\hat{t}_R},\qquad \tau_a=t\mathrm{Pe}=\frac{\hat{t}}{\hat{t}_A}. \tag{18}$$

Furthermore, it represents the concentration $c_\varepsilon(\mathbf{x},t)$ in Eq. (10), or its counterpart in Eq. (14), as $c_\varepsilon(\mathbf{x},t):=c(\mathbf{x},\mathbf{y},t,\tau_r,\tau_a)$. The latter is expanded into an asymptotic series in powers of ε,

$$c(\mathbf{x},\mathbf{y},t,\tau_r,\tau_a)=\sum_{m=0}^{\infty}\varepsilon^m c_m(\mathbf{x},\mathbf{y},t,\tau_r,\tau_a), \tag{19}$$

wherein $c_m(\mathbf{x},\mathbf{y},t,\tau_r,\tau_a)$ $(m=0,1,\ldots)$ are Y-periodic in $\mathbf{y}$. Finally, we set

$$\mathrm{Pe}=\varepsilon^{-\alpha}\quad\text{and}\quad \mathrm{Da}=\varepsilon^{\beta}, \tag{20}$$

with the exponents α and β determining the system behavior. For example, transport due to advection and dispersion at the pore scale is not homogenizable if $\alpha \geq 2$ (Auriault and Adler, 1995, Section 3.5, Table 1).

We show in the Appendix that pore-scale reactive transport processes described by Eqs. (10)–(11) can be homogenized, i.e., approximated up to order ε^2 with an effective ADRE

$$\phi \frac{\partial \langle c \rangle_{\mathcal{B}}}{\partial t} = \nabla \cdot (\mathbf{D}^* \nabla \langle c \rangle_{\mathcal{B}} - \mathrm{Pe} \langle c \rangle_{\mathcal{B}} \langle \mathbf{v} \rangle) - \varepsilon^{-1} \phi \mathrm{Da} \mathcal{K}^* (\langle c \rangle_{\mathcal{B}}^a - 1), \quad \mathbf{x} \in \Omega, \tag{21}$$

provided the following conditions are met:

1) $\varepsilon \ll 1$,
2) $\mathrm{Pe} < \varepsilon^{-2}$,
3) $\mathrm{Da}/\mathrm{Pe} < \varepsilon$,
4) $\mathrm{Da} < 1$,
5) $\langle \chi \rangle_{\Gamma} \approx \langle \chi \rangle_{\mathcal{B}}$.

In Eq. (21), the dimensionless effective reaction rate constant $\mathcal{K}^*$ is determined by the pore geometry,

$$\mathcal{K}^* = \frac{|\Gamma|}{|\mathcal{B}|}, \tag{22}$$

and the dispersion tensor $\mathbf{D}^*$ is given by

$$\mathbf{D}^* = \langle \mathbf{D}(\mathbf{I} + \nabla_{\mathrm{y}} \chi) \rangle + \varepsilon \mathrm{Pe} \langle \chi \mathbf{k} \rangle \nabla_{\mathrm{x}} p_0. \tag{23}$$

The closure variable $\chi(\mathbf{y})$ has zero mean, $\langle \chi \rangle = \mathbf{0}$, and is defined as a solution of the local problem

$$-\nabla_{\mathrm{y}} \cdot \mathbf{D}(\nabla_{\mathrm{y}} \chi + \mathbf{I}) + \varepsilon \mathrm{Pe} \mathbf{v}_0 \nabla_{\mathrm{y}} \chi = \varepsilon \mathrm{Pe}(\langle \mathbf{v}_0 \rangle_{\mathcal{B}} - \mathbf{v}_0), \mathbf{y} \in \mathcal{B}; \tag{24a}$$

$$-\mathbf{n} \cdot \mathbf{D}(\nabla_{\mathrm{y}} \chi + \mathbf{I}) = 0, \mathbf{y} \in \Gamma; \tag{24b}$$

where $\mathbf{v}_0 = -\mathbf{k} \cdot \nabla_{\mathrm{x}} p_0$ and the pressure p_0 is a solution of the effective flow Eq. (16).

Constraints 1)–4) ensure the separation of scales. While constraint 1) is almost always met in practical applications, the rest of them depend on the relative importance of advective, diffusive, and reactive mechanisms of transport. These conditions are summarized in the phase diagram in Fig. 1, where the line $\beta = 0$ corresponds to $\mathrm{Da} = 1$ and the half-space $\beta > 0$ to $\mathrm{Da} < 1$ because $\varepsilon < 1$; the line $\alpha = 2$ corresponds to $\mathrm{Pe} = \varepsilon^{-2}$ and the half-space $\alpha < 2$ corresponds to $\mathrm{Pe} < \varepsilon^{-2}$; the line $\alpha + \beta = 1$ corresponds to $\mathrm{Da}/\mathrm{Pe} = \varepsilon$; and the half-space underneath this line corresponds to $\mathrm{Da}/\mathrm{Pe} < \varepsilon$. Constraints 3) and 4) require that either diffusion or advection–diffusion dominate reactions at the pore scale. This allows one to decouple the pore- and continuum-scale descriptions (see Appendix A.2). Constraint 5) is not required for scale separation, but facilitates the derivation of the effective parameters (22) and (23). As shown in Appendix A.3, this constraint allows one to interchange the surface and volume averages, $\langle c_1 \rangle_{\Gamma} \approx \langle c_1 \rangle_{\mathcal{B}}$, within errors on the order of ε^2.

The results above generalize the conclusions of the analysis of reactive–diffusive transport (Battiato et al., 2009), which relied on the method of volume averaging. While using different upscaling approaches, both analyses provide the same bound on the Damköhler number Da in the absence of advection. The effective reaction rate $\mathcal{K}^*$ for heterogeneous reactions (22) is likewise consistent with that obtained in (Battiato et al., 2009). This suggests that the conditions for the validity and breakdown of continuum models of reactive transport presented in the phase diagram in Fig. 1 are universal and independent of an upscaling method. Finally, these upscaling results justify the use of reaction terms similar to the one in Eq. (21) in continuum models of precipitation and dissolution processes in porous media (e.g., Broyda et al., 2010; Lichtner and Tartakovsky 2003; Tartakovsky et al., 2009).

4. Special cases

In this section, we explore specific flow and transport regimes under which general forms of the upscaled Eq. (21) and the closure problem (24) can be simplified. Specifically, we demonstrate how the conditions identified in (Auriault and Adler, 1995) for advection–dispersion transport of conservative solutes can be derived from Eqs. (21) and (24). As briefly mentioned in Section 2 and thoroughly discussed in Appendix A.2, constraints 3) and 4) ensure that reactions are negligible at the pore level. Hence, the following regimes are either diffusion or advection–diffusion dominated at the pore scale.

4.1. Transport regime with $\varepsilon \leq \mathrm{Pe} < 1$

In this regime ($-1 \leq \alpha < 0$), diffusion dominates advection at the macro-scale and Eq. (21) reduces to a dispersion–reaction equation

$$\varepsilon \phi \frac{\partial \langle c \rangle_{\mathcal{B}}}{\partial t} = \varepsilon \nabla_{\mathrm{x}} \cdot (\mathbf{D}^* \nabla_{\mathrm{x}} \langle c \rangle_{\mathcal{B}}) - \mathrm{Da} \phi \mathcal{K}^* (\langle c \rangle_{\mathcal{B}}^a - 1), \tag{25}$$

where $\mathbf{D}^* = \langle \mathbf{D}(\mathbf{I} + \nabla_{\mathrm{y}} \chi) \rangle$ and the closure problem (24) simplifies to

$$-\nabla_{\mathrm{y}} \cdot \mathbf{D}(\nabla_{\mathrm{y}} \chi + \mathbf{I}) = \mathbf{0}, \quad \mathbf{y} \in \mathcal{B}; \tag{26a}$$

$$\mathbf{n} \cdot \mathbf{D}(\nabla_{\mathrm{y}} \chi + \mathbf{I}) = \mathbf{0}, \quad \mathbf{y} \in \Gamma. \tag{26b}$$

The magnitude of the Damköhler number Da determines the effects of chemical reactions on transport.

4.1.1. Diffusion dominates reactions, $\mathrm{Da} < \varepsilon$

In this regime ($\beta > 1$, the dot-patterned region in Fig. 1), the diffusion term in the macro-scale Eq. (25) dominates the reaction term, so that Eq. (25) simplifies to a non-reactive dispersion equation

$$\phi \frac{\partial \langle c \rangle_{\mathcal{B}}}{\partial t} = \nabla \cdot (\mathbf{D}^* \nabla \langle c \rangle_{\mathcal{B}}), \tag{27}$$

which coincides with Eqs. (45) and (46) in (Auriault and Adler, 1995).

4.1.2. Diffusion and reaction are comparable, $\mathrm{Da} = \varepsilon$

In this regime ($\beta = 1$, the red dot in Fig. 1), the reaction term in the effective Eq. (25) cannot be neglected. Reactive transport at the macro-scale is described by the dispersion-reaction Eq. (25).

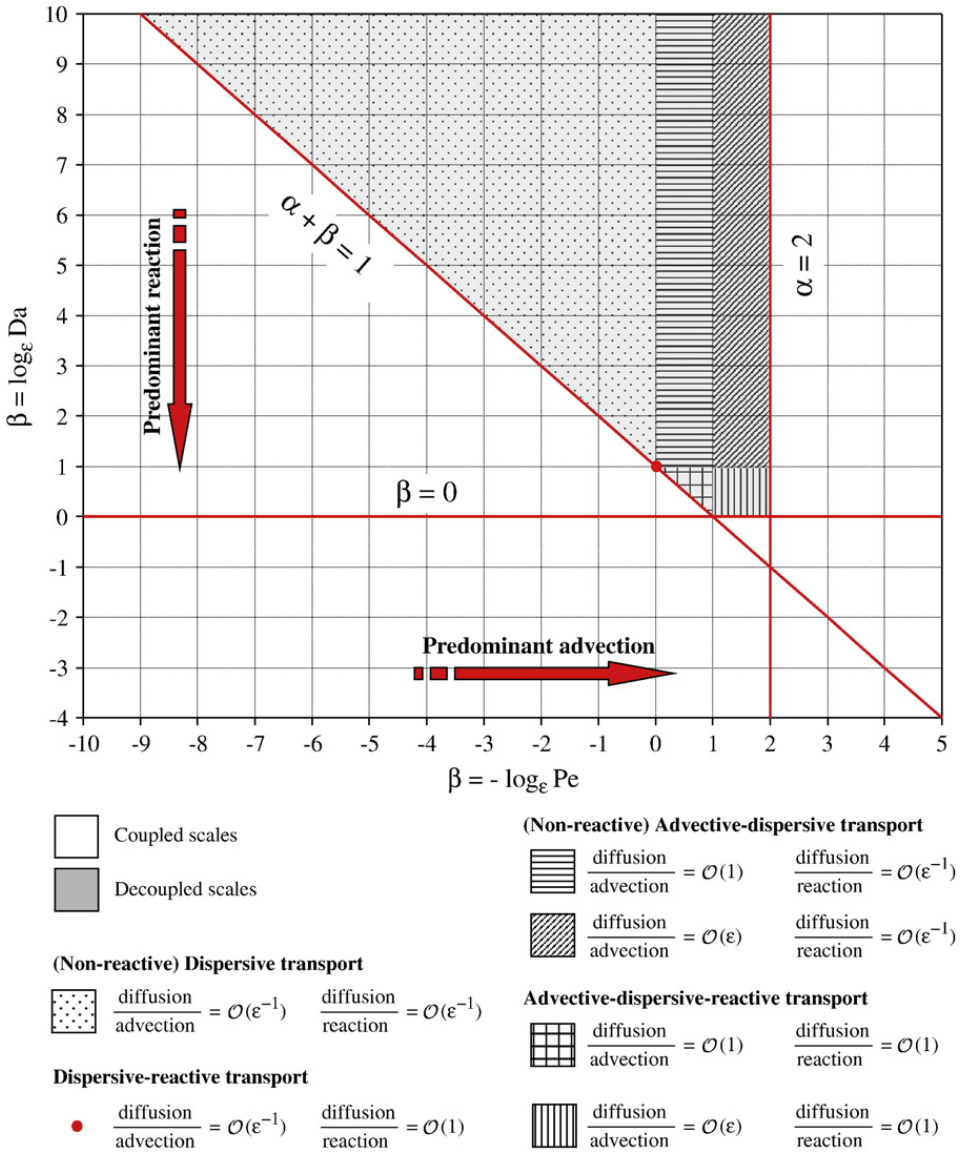

Fig. 1. Phase diagram indicating the range of applicability of macroscopic equations for the advection–reaction–diffusion system (10)–(11) in terms of Pe and Da. The grey region identifies the sufficient conditions under which the macroscopic equations hold. In the white region, macro- and micro-scale problems are coupled and have to be solved simultaneously. Also identified are different transport regimes depending on the order of magnitude of Pe and Da. Diffusion, advection, and reaction are of the same order of magnitude at the point $(\alpha, \beta) = (1, 0)$.

4.2. Transport regime with $1 \le Pe < \varepsilon^{-1}$

In this regime ($0 \le \alpha < 1$), the effects of advection and diffusion at the macro-scale are of the same order. While the advective term can be neglected in the closure problem (24), it has to be retained in the effective Eq. (21). Consequently, reactive transport at the macro-scale is described by the advection–dispersion-reaction Eq. (21) with the effective dispersion tensor $\mathbf{D}^* = \langle \mathbf{D}(\mathbf{I} + \nabla_y \boldsymbol{\chi}) \rangle$, in which the closure variable $\boldsymbol{\chi}(\mathbf{y})$ is a solution of Eqs. (26).

4.2.1. Diffusion and advection dominate reactions, $Da < \varepsilon$

In this regime ($\beta > 1$, the horizontal-line-patterned region in Fig. 1), Eq. (21) reduces to a non-reactive advection–dispersion equation

$$\phi \frac{\partial \langle c \rangle_{\mathcal{B}}}{\partial t} = \nabla \cdot \left(\mathbf{D}^* \nabla \langle c \rangle_{\mathcal{B}} \right) - \mathrm{Pe} \nabla \cdot \left(\langle c \rangle_{\mathcal{B}} \langle \mathbf{v} \rangle \right), \tag{28}$$

and the closure problem is given by Eqs. (26). This upscaled model is identical to that derived in (Auriault and Adler, 1995, Eqs. 46 and 51) for advection–dispersion transport of passive solutes.

4.2.2. Diffusion and reactions are comparable, $\varepsilon \le Da < 1$

In this regime ($0 < \beta \le 1$, the square-patterned region in Fig. 1), pore-scale transport is still diffusion driven, and $\boldsymbol{\chi}$ and $\mathbf{D}^*$ are defined by Eqs. (26) and $\mathbf{D}^* = \langle \mathbf{D}(\mathbf{I} + \nabla_y \boldsymbol{\chi}) \rangle$, respectively. At the macro-scale, the reaction term is not negligible, so that the effective transport Eq. (21) is to be used.

4.3. Transport regime with $\varepsilon^{-1} \le Pe < \varepsilon^{-2}$

In this regime ($1 \le \alpha < 2$), advection dominates diffusion at the macro-scale and transport is described by Eq. (21). Since at the pore scale these two transport mechanisms are of the

same order, the effective dispersion tensor $\mathbf{D}^*$ is given by Eq. (23) and the closure variable χ is obtained by solving the cell problem (24). The magnitude of the Damköhler number Da determines the following sub-regimes.

4.3.1. Diffusion dominates reactions, $Da<\varepsilon$

In this regime ($\beta>1$, the diagonal-line-patterned region in Fig. 1), diffusion dominates reactions at the continuum scale. The effective transport Eq. (21) reduces to Eq. (28) wherein the dispersion tensor $\mathbf{D}^*$ is given by Eq. (23). The latter transport model coincides with that derived in (Auriault and Adler, 1995, Eqs. 61, 65, 68).

4.3.2. Diffusion and reactions are comparable, $\varepsilon\leq Da<1$

In this regime ($0<\beta\leq 1$, the vertical-line-patterned region in Fig. 1), transport is advection-dominated (reactions are negligible) at the pore-scale, but diffusion and reactions at the macro-scale are of the same order of magnitude. Hence, both the effective dispersion tensor $\mathbf{D}^*$ and the closure variable χ are defined as in Section 4.3.1, and the effective transport model is the advection–dispersion-reaction Eq. (21).

5. Conclusions

Reactive transport in porous media is a complex nonlinear phenomenon that often involves both homogeneous and heterogeneous reactions of (bio-)chemical species dissolved in a liquid phase. The relative importance of advection, molecular diffusion, and reactions (three key pore-scale transport mechanisms) is quantified by the Péclet (Pe) and Damköhler (Da) numbers. We considered transport of a solute that undergoes nonlinear heterogeneous reactions: after reaching a threshold concentration, it precipitates on the solid matrix to form a crystalline solid. The main goal of this study was to establish sufficient conditions under which macroscopic advection–dispersion-reaction equations (ADREs) provide an accurate description of pore-scale processes. To accomplish this, we used multiple-scale expansions to upscale to the continuum (Darcy) scale a pore-scale advection–diffusion equation with reactions entering through a boundary condition on the fluid–solid interfaces. Our analysis leads to the following major conclusions.

1. The range of applicability of macroscopic ADREs and various transport regimes can be described with a phase diagram in the (Da, Pe)-space (Fig. 1). The latter is parameterized with the scale-separation parameter ε that is defined as the ratio of characteristic lengths associated with the pore- and macro-scales.
2. This phase diagram reveals that transport phenomena dominated at the pore scale by reaction processes do not lend themselves to macroscopic (upscaled) descriptions. Under these conditions, the validity of assumptions and approximations underlying macroscopic ADREs, such as Eq. (21), cannot be ascertained a priori.
3. The constraints on Pe and Da obtained in the present analysis are consistent with those derived for diffusion-reaction transport in (Battiato et al., 2009) by means of volume averaging, which suggests that these results are universal, i.e., are independent of the choice of an upscaling technique.
4. The constraints on Pe derived in (Auriault and Adler, 1995) follow from our formulation as special cases.
5. For transport regimes, in which continuum (Darcy-scale) equations breakdown, nonlocal (integro-differential) or hybrid pore-scale/continuum-scale models should be used, as they provide a more rigorous alternative to classical upscaled models based on closure assumptions and approximations.

In follow-up studies we will develop hybrid algorithms that couple a pore-scale model in the regions where the validity of macro-scale models cannot be ascertained a priori with continuum descriptions elsewhere in a computational domain.

Acknowledgement

This research was supported by the Office of Science of the U.S. Department of Energy (DOE) under the Scientific Discovery through Advanced Computing (SciDAC).

Appendix A. Homogenization of transport equations

Replacing $c_\varepsilon(\mathbf{x}, t)$ with $c(\mathbf{x}, \mathbf{y}, t, \tau_r, \tau_a)$ gives the following relations for the spatial and temporal derivatives,

$$\nabla c_\varepsilon = \nabla_{\mathbf{x}} c + \frac{1}{\varepsilon}\nabla_{\mathbf{y}} c \tag{A.1}$$

and

$$\frac{\partial c_\varepsilon}{\partial t} = \frac{\partial c}{\partial t} + \mathrm{Da}\frac{\partial c}{\partial \tau_r} + \mathrm{Pe}\frac{\partial c}{\partial \tau_a}. \tag{A.2}$$

Substitution of Eqs. (A.1) and (A.2) into Eqs. (10) and (11) yields

$$\begin{aligned}&\frac{\partial c}{\partial t} + \mathrm{Da}\frac{\partial c}{\partial \tau_r} + \mathrm{Pe}\frac{\partial c}{\partial \tau_a} + \nabla_{\mathbf{x}}\cdot\left[-\mathbf{D}\left(\nabla_{\mathbf{x}} c + \varepsilon^{-1}\nabla_{\mathbf{y}} c\right) + \mathrm{Pe}\mathbf{v}c\right]\\ &\quad + \varepsilon^{-1}\nabla_{\mathbf{y}}\cdot\left[-\mathbf{D}\left(\nabla_{\mathbf{x}} c + \varepsilon^{-1}\nabla_{\mathbf{y}} c\right) + \mathrm{Pe}\mathbf{v}c\right] = 0, \qquad \mathbf{y}\in\mathcal{B}\end{aligned} \tag{A.3}$$

and

$$-\mathbf{n}\cdot\mathbf{D}\left(\nabla_{\mathbf{x}} c + \varepsilon^{-1}\nabla_{\mathbf{y}} c\right) = \mathrm{Da}\left(c^a - 1\right), \qquad \mathbf{y}\in\Gamma, \tag{A.4}$$

respectively. Substituting Eqs. (19) and (20) into Eq. (A.3) leads to

$$\begin{aligned}&\varepsilon^{-2}\left[\nabla_{\mathbf{y}}\cdot\left(-\mathbf{D}\nabla_{\mathbf{y}} c_0 + \varepsilon^{1-\alpha} c_0\mathbf{v}_0\right)\right]\\ &\quad + \varepsilon^{-1}\left\{-\nabla_{\mathbf{x}}\cdot\mathbf{D}\nabla_{\mathbf{y}} c_0 - \nabla_{\mathbf{y}}\cdot\mathbf{D}\left(\nabla_{\mathbf{y}} c_1 + \nabla_{\mathbf{x}} c_0\right)\right.\\ &\quad \left. + \varepsilon^{1-\alpha}\left[\frac{\partial c_0}{\partial \tau_a} + \varepsilon^{\alpha+\beta}\frac{\partial c_0}{\partial \tau_r} + \nabla_{\mathbf{x}}\cdot(c_0\mathbf{v}_0) + \nabla_{\mathbf{y}}\cdot(c_1\mathbf{v}_0 + c_0\mathbf{v}_1)\right]\right\}\\ &\quad + \varepsilon^{0}\left\{\frac{\partial c_0}{\partial t} - \nabla_{\mathbf{x}}\cdot\mathbf{D}\left(\nabla_{\mathbf{x}} c_0 + \nabla_{\mathbf{y}} c_1\right) - \nabla_{\mathbf{y}}\cdot\mathbf{D}\left(\nabla_{\mathbf{x}} c_1 + \nabla_{\mathbf{y}} c_2\right)\right.\\ &\quad + \varepsilon^{1-\alpha}\left[\frac{\partial c_1}{\partial \tau_a} + \varepsilon^{\alpha+\beta}\frac{\partial c_1}{\partial \tau_r} + \nabla_{\mathbf{x}}\cdot(c_1\mathbf{v}_0 + c_0\mathbf{v}_1)\right.\\ &\quad \left.\left. + \nabla_{\mathbf{y}}\cdot(c_1\mathbf{v}_1 + c_0\mathbf{v}_2 + c_2\mathbf{v}_0)\right]\right\} = \mathcal{O}(\varepsilon), \qquad \mathbf{y}\in\mathcal{B}.\end{aligned} \tag{A.5}$$

Similarly, boundary condition (A.4) can be written as

$$\varepsilon^{-1}\left(-\mathbf{n}\cdot\mathbf{D}\nabla_{\mathbf{y}}c_0\right)+\varepsilon^{0}\left[-\mathbf{n}\cdot\mathbf{D}\left(\nabla_{\mathbf{x}}c_0+\nabla_{\mathbf{y}}c_1\right)-\varepsilon^{\beta}(c_0^a-1)\right]+\varepsilon\left[-\mathbf{n}\cdot\mathbf{D}\left(\nabla_{\mathbf{x}}c_1+\nabla_{\mathbf{y}}c_2\right)-\varepsilon^{\beta}c_0^{a-1}c_1\right]=\mathcal{O}\left(\varepsilon^2\right),\qquad \mathbf{y}\in\Gamma. \tag{A.6}$$

Next, we collect the terms of like-powers in ε under condition that $\alpha<2$, which is required for the homogenizability of the advection–dispersion equation (Auriault and Adler, 1995, Section 3.5, Table 1).

A.1. Terms of order $\mathcal{O}(\varepsilon^{-2})$

Collecting the leading-order terms in Eqs. (A.5) and (A.6), we obtain a partial differential equation (PDE),

$$\nabla_{\mathbf{y}}\cdot\left(-\mathbf{D}\nabla_{\mathbf{y}}c_0+\varepsilon^{1-\alpha}c_0\mathbf{v}_0\right)=0,\qquad \mathbf{y}\in\mathcal{B}, \tag{A.7}$$

subject to the boundary condition

$$-\mathbf{n}\cdot\left(\mathbf{D}\nabla_{\mathbf{y}}c_0\right)=0,\qquad \mathbf{y}\in\Gamma. \tag{A.8}$$

The homogeneity of both Eqs. (A.7) and (A.8) ensures that this boundary-value problem has a trivial solution, i.e., that c_0 is independent of $\mathbf{y}$,

$$c_0=c_0(\mathbf{x},t,\tau_r,\tau_a),\qquad \text{for any } \alpha<2. \tag{A.9}$$

Note that this result does not require the convoluted analysis presented in (Auriault and Adler, 1995, Eqs. 48).

A.2. Terms of order $\mathcal{O}(\varepsilon^{-1})$

Since $\nabla_{\mathbf{y}}c_0\equiv 0$, the next order terms in Eqs. (A.5) and (A.6) give rise to a PDE

$$-\nabla_{\mathbf{y}}\cdot\mathbf{D}\left(\nabla_{\mathbf{y}}c_1+\nabla_{\mathbf{x}}c_0\right)+\varepsilon^{1-\alpha}\left[\frac{\partial c_0}{\partial\tau_a}+\varepsilon^{\alpha+\beta}\frac{\partial c_0}{\partial\tau_r}+\nabla_{\mathbf{x}}\cdot(c_0\mathbf{v}_0)+\nabla_{\mathbf{y}}\cdot(c_1\mathbf{v}_0+c_0\mathbf{v}_1)\right]=0,\qquad \mathbf{y}\in\mathcal{B}. \tag{A.10}$$

subject to the boundary condition

$$-\mathbf{n}\cdot\mathbf{D}\left(\nabla_{\mathbf{x}}c_0+\nabla_{\mathbf{y}}c_1\right)-\varepsilon^{\beta}(c_0^a-1)=0,\qquad \mathbf{y}\in\Gamma. \tag{A.11}$$

Integrating Eq. (A.10) over $\mathcal{B}$ with respect to $\mathbf{y}$, while accounting for the no-slip boundary condition on Γ, the boundary condition (A.11), and the periodicity of the coefficients on the external boundary of the unit cell ∂Y, we obtain

$$\varepsilon^{1-\alpha}\frac{\partial c_o}{\partial\tau_a}+\varepsilon^{1+\beta}\frac{\partial c_0}{\partial\tau_r}=-\varepsilon^{1-\alpha}\nabla_{\mathbf{x}}\cdot(c_0\langle\mathbf{v}_0\rangle_{\mathcal{B}})-\varepsilon^{\beta}\mathcal{K}^*(c_0^a-1) \tag{A.12}$$

where $\mathcal{K}^*$ is defined by Eq. (22).

Combining Eq. (A.12) with Eq. (A.10) to eliminate the temporal derivatives, we obtain

$$\varepsilon^{1-\alpha}\left[-\nabla_{\mathbf{x}}\cdot(c_0\langle\mathbf{v}_0\rangle_{\mathcal{B}})-\varepsilon^{\alpha+\beta-1}\mathcal{K}^*(c_0^a-1)+\nabla_{\mathbf{x}}\cdot(c_0\mathbf{v}_0)\right]+\nabla_{\mathbf{y}}\cdot(c_1\mathbf{v}_0+c_0\mathbf{v}_1)-\nabla_{\mathbf{y}}\cdot\mathbf{D}\left(\nabla_{\mathbf{y}}c_1+\nabla_{\mathbf{x}}c_0\right)=0. \tag{A.13}$$

Since $\nabla_{\mathbf{y}}\cdot\mathbf{v}_0=0$ (Auriault and Adler, 1995, Eq. 20), $\nabla_{\mathbf{x}}\cdot\langle\mathbf{v}_0\rangle_{\mathcal{B}}=0$ (Auriault and Adler, 1995, Eq. 26), $\nabla_{\mathbf{y}}\cdot\mathbf{v}_1+\nabla_{\mathbf{x}}\cdot\mathbf{v}_0=0$ (Auriault and Adler, 1995, Eq. 25), and $\nabla_{\mathbf{y}}c_0=0$ from Eq. (A.9), this gives

$$\varepsilon^{1-\alpha}[(\mathbf{v}_0-\langle\mathbf{v}_0\rangle_{\mathcal{B}})\nabla_{\mathbf{x}}\cdot c_0-\varepsilon^{\alpha+\beta-1}\mathcal{K}^*(c_0^a-1)+\mathbf{v}_0\nabla_{\mathbf{y}}\cdot c_1]-\nabla_{\mathbf{y}}\cdot\mathbf{D}(\nabla_{\mathbf{y}}c_1+\nabla_{\mathbf{x}}c_0)=0. \tag{A.14}$$

Eqs. (A.14) and (A.11) form a boundary-value problem for c_1. Following (Auriault and Adler, 1995, Eq. 40) and (Hornung, 1997, p. 10, Eqs. 3.6–3.7), we look for a solution in the form

$$c_1(\mathbf{x},\mathbf{y},t,\tau_r,\tau_a)=\boldsymbol{\chi}(\mathbf{y})\cdot\nabla_{\mathbf{x}}c_0(\mathbf{x},t,\tau_r,\tau_a)+\bar{c}_1(\mathbf{x},t,\tau_r,\tau_a). \tag{A.15}$$

Substitution of Eq. (A.15) into Eqs. (A.14) and (A.11) leads to the following cell problem for the closure variable $\boldsymbol{\chi}(\mathbf{y})$:

$$\left[-\nabla_{\mathbf{y}}\cdot\mathbf{D}\left(\nabla_{\mathbf{y}}\boldsymbol{\chi}+\mathbf{I}\right)+\varepsilon^{1-\alpha}\mathbf{v}_0\cdot\nabla_{\mathbf{y}}\boldsymbol{\chi}\right]\cdot\nabla_{\mathbf{x}}c_0=\varepsilon^{1-\alpha}(\langle\mathbf{v}_0\rangle_{\mathcal{B}}-\mathbf{v}_0)\cdot\nabla_{\mathbf{x}}c_0+\varepsilon^{\beta}\mathcal{K}^*(c_0^a-1),\qquad \mathbf{y}\in\mathcal{B}; \tag{A.16a}$$

subject to $\langle\boldsymbol{\chi}\rangle=0$ and

$$-\left[\mathbf{n}\cdot\mathbf{D}\left(\nabla_{\mathbf{y}}\boldsymbol{\chi}+\mathbf{I}\right)\right]\cdot\nabla_{\mathbf{x}}c_0=\varepsilon^{\beta}(c_0^a-1),\qquad \mathbf{y}\in\Gamma. \tag{A.16b}$$

Note that $\boldsymbol{\chi}(\mathbf{y})$ is a Y-periodic vector field.

The boundary-value problem (A.16) couples the pore scale with the continuum scale, in the sense that the closure variable $\boldsymbol{\chi}(\mathbf{y})$—a solution of the pore-scale cell problem (A.16)—is influenced by the continuum scale through its dependence on the macroscopic concentration $c_0(\mathbf{x})$. This coupling is incompatible with the general representation (A.15). This inconsistency is resolved by imposing the following constraints on the exponents α and β.

We start with the boundary condition in Eq. (A.16b), whose left-hand-side is of order ε^0. If we chose $\beta>0$, then the right-hand-side, which is of order ε^{β}, can be neglected since $\varepsilon\ll 1$ (Constraint 1 of Section 3.2). Next, we observe that for the term $\varepsilon^{\beta}\mathcal{K}^*(c_0^a-1)$ to be negligible relative to the smallest term in Eq. (A.16a) it is necessary that $\beta>\max\{0,1-\alpha\}$. Since homogenizability of pore-scale advection–diffusion transport of a conservative solute requires that $\alpha<2$ (Auriault and Adler, 1995, Section 3.5, Table 1), this condition yields either $\beta+\alpha>1$ if $\alpha<1$ or $\beta>0$ if $1<\alpha<2$.

The selection of proper α and β ensures that $\boldsymbol{\chi}$ is independent of c_0. The dependence of $\boldsymbol{\chi}$ on $\nabla_{\mathbf{x}}c_0$ is eliminated by defining $\boldsymbol{\chi}$ as a solution of the related cell problem (24). Finally, recalling the definitions of Da and Pe in Eq. (20)

allows us to reformulate the conditions on α and β in the form of constraints 2)–4) of Section 3.2.

Having identified the conditions that guarantee homogenizability, we proceed to derive the effective transport Eq. (21).

A.3. Terms of order $\mathcal{O}(\varepsilon^0)$

Collecting the zeroth-order terms in Eqs. (A.5) and (A.6), we obtain

$$\frac{\partial c_0}{\partial t} - \nabla_{\mathbf{x}}\cdot\mathbf{D}\left(\nabla_{\mathbf{x}}c_0 + \nabla_{\mathbf{y}}c_1\right) - \nabla_{\mathbf{y}}\cdot\mathbf{D}\left(\nabla_{\mathbf{x}}c_1 + \nabla_{\mathbf{y}}c_2\right) + \varepsilon^{1-\alpha}\left[\frac{\partial c_1}{\partial \tau_a} + \varepsilon^{\alpha+\beta}\frac{\partial c_1}{\partial \tau_r} + \nabla_{\mathbf{x}}\cdot(c_1\mathbf{v}_0 + c_0\mathbf{v}_1) + \nabla_{\mathbf{y}}\cdot(c_1\mathbf{v}_1 + c_0\mathbf{v}_2 + c_2\mathbf{v}_0)\right] = 0, \qquad \mathbf{y}\in\mathcal{B}, \tag{A.17}$$

with the boundary condition

$$-\mathbf{n}\cdot\mathbf{D}\left(\nabla_{\mathbf{x}}c_1 + \nabla_{\mathbf{y}}c_2\right) - a\varepsilon^{\beta}c_0^{a-1}c_1 = 0, \qquad \mathbf{y}\in\Gamma. \tag{A.18}$$

Integrating Eq. (A.17) over $\mathcal{B}$ with respect to $\mathbf{y}$ and using the boundary condition (A.18) leads to

$$\frac{\partial\langle c_0\rangle_{\mathcal{B}}}{\partial t} - \nabla_{\mathbf{x}}\cdot\left(\phi^{-1}\mathbf{D}^{**}\nabla_{\mathbf{x}}c_0\right) + a\varepsilon^{\beta}\mathcal{K}^*c_0^{a-1}\langle c_1\rangle_{\Gamma} + \varepsilon^{1-\alpha}\left[\frac{\partial\langle c_1\rangle_{\mathcal{B}}}{\partial\tau_a} + \varepsilon^{\alpha+\beta}\frac{\partial\langle c_1\rangle_{\mathcal{B}}}{\partial\tau_r} + \nabla_{\mathbf{x}}\cdot\left(\langle c_1\mathbf{v}_0\rangle_{\mathcal{B}} + c_0\langle\mathbf{v}_1\rangle_{\mathcal{B}}\right)\right] = 0 \tag{A.19}$$

where $\mathbf{D}^{**} = \langle\mathbf{D}(\mathbf{I} + \nabla_{\mathbf{y}}\boldsymbol{\chi})\rangle$. Combining Eq. (A.19) with Eq. (A.15), while making use of (A.18), the definition $|\Gamma|\langle c_1\rangle_{\Gamma} = \int_{\Gamma}c_1 d\mathbf{y}$, and the relations $c_0 = \langle c_0\rangle_{\mathcal{B}}$ and $\mathbf{v}_0 = -\mathbf{k}(\mathbf{y})\cdot\nabla_{\mathbf{x}}p_0$ (Auriault and Adler, 1995, Eq. 21), we obtain

$$\frac{\partial\langle c_0\rangle_{\mathcal{B}}}{\partial t} + \varepsilon^{1-\alpha}\frac{\partial\langle c_1\rangle_{\mathcal{B}}}{\partial\tau_a} + \varepsilon^{1+\beta}\frac{\partial\langle c_1\rangle_{\mathcal{B}}}{\partial\tau_r} = \nabla_{\mathbf{x}}\cdot\left(\phi^{-1}\mathbf{D}^*\nabla_{\mathbf{x}}c_0\right) - a\varepsilon^{\beta}\mathcal{K}^*c_0^{a-1}\langle c_1\rangle_{\Gamma} - \phi^{-1}\varepsilon^{1-\alpha}\nabla_{\mathbf{x}}\cdot\left(c_0\langle\mathbf{v}_1\rangle + \bar{c}_1\langle\mathbf{v}_0\rangle\right), \tag{A.20}$$

where $\mathbf{D}^*(\mathbf{x})$ is given by Eq. (23).

Next we recall that

$$\langle c\rangle_{\mathcal{B}} = \langle c_{\varepsilon}\rangle_{\mathcal{B}} = \langle c_0\rangle_{\mathcal{B}} + \varepsilon\langle c_1\rangle_{\mathcal{B}} + \mathcal{O}\left(\varepsilon^2\right). \tag{A.21}$$

Multiplying the temporal derivative of Eq. (A.21) with ε, using Eq. (20), and recognizing that $\partial\langle c_1\rangle_{\mathcal{B}}/\partial t$ is of order ε^2, we obtain

$$\varepsilon\frac{\partial\langle c\rangle_{\mathcal{B}}}{\partial t} = \left(\varepsilon^{\beta+1}\frac{\partial\langle c_0\rangle_{\mathcal{B}}}{\partial\tau_r} + \varepsilon^{1-\alpha}\frac{\partial\langle c_0\rangle_{\mathcal{B}}}{\partial\tau_a}\right) + \varepsilon\left(\frac{\partial\langle c_0\rangle_{\mathcal{B}}}{\partial t} + \varepsilon^{\beta+1}\frac{\partial\langle c_1\rangle_{\mathcal{B}}}{\partial\tau_r} + \varepsilon^{1-\alpha}\frac{\partial\langle c_1\rangle_{\mathcal{B}}}{\partial\tau_a}\right) + \mathcal{O}\left(\varepsilon^2\right). \tag{A.22}$$

Multiplying Eq. (A.20) with ε, adding the result to Eq. (A.12), and using Eq. (A.22), we obtain

$$\varepsilon\frac{\partial\langle c\rangle_{\mathcal{B}}}{\partial t} = \varepsilon\nabla_{\mathbf{x}}\cdot\left(\phi^{-1}\mathbf{D}^*\nabla\langle c_0\rangle_{\mathcal{B}}\right) - \phi^{-1}\varepsilon^{1-\alpha}\nabla\cdot\left(\langle c_0\rangle\langle\mathbf{v}_0\rangle_{\mathcal{B}} + \varepsilon c_0\langle\mathbf{v}_1\rangle + \varepsilon\,\bar{c}_1\langle\mathbf{v}_0\rangle\right) + \varepsilon^{\beta}\mathcal{K}^*\left(1 - c_0^a - a\varepsilon c_0^{a-1}\langle c_1\rangle_{\Gamma}\right). \tag{A.23}$$

Since $\bar{c}_1 = \langle c_1\rangle_{\mathcal{B}}$ (i.e., $\langle\chi\rangle = \phi\langle\chi\rangle_{\mathcal{B}} = 0$) and $\langle c_0\rangle_{\mathcal{B}}\langle\mathbf{v}_0\rangle = \langle c_0\rangle_{\mathcal{B}}\langle\mathbf{v}_0\rangle$, an expansion

$$\langle c\rangle_{\mathcal{B}}\langle\mathbf{v}\rangle = \langle c_0\rangle_{\mathcal{B}}\langle\mathbf{v}_0\rangle + \varepsilon\langle c_0\rangle_{\mathcal{B}}\langle\mathbf{v}_1\rangle + \varepsilon\langle c_1\rangle_{\mathcal{B}}\langle\mathbf{v}_0\rangle + \mathcal{O}\left(\varepsilon^2\right) \tag{A.24}$$

gives

$$\langle c\rangle_{\mathcal{B}}\langle\mathbf{v}\rangle = \langle c_0\rangle\langle\mathbf{v}_0\rangle_{\mathcal{B}} + \varepsilon c_0\langle\mathbf{v}_1\rangle + \varepsilon\bar{c}_1\langle\mathbf{v}_0\rangle + \mathcal{O}\left(\varepsilon^2\right). \tag{A.25}$$

Combining this result with an expansion $\varepsilon\langle c\rangle_{\mathcal{B}} = \varepsilon\langle c_0\rangle_{\mathcal{B}} + \mathcal{O}(\varepsilon^2) = \varepsilon c_0 + \mathcal{O}(\varepsilon^2)$ allows one to express the diffusive term in Eq. (A.23) in terms of $\langle c\rangle_{\mathcal{B}}$, which leads to

$$\phi\frac{\partial\langle c\rangle_{\mathcal{B}}}{\partial t} = \nabla_{\mathbf{x}}\cdot\left(\mathbf{D}^*\nabla_{\mathbf{x}}\langle c\rangle_{\mathcal{B}}\right) - \mathrm{Pe}\nabla_{\mathbf{x}}\cdot\left(\langle c\rangle_{\mathcal{B}}\langle\mathbf{v}\rangle\right) + \varepsilon^{-1}\mathrm{Da}\phi\,\mathcal{K}^*\left(1 - \langle c_0\rangle_{\mathcal{B}}^a - a\varepsilon\langle c_0\rangle_{\mathcal{B}}^{a-1}\langle c_1\rangle_{\Gamma}\right). \tag{A.26}$$

If one can assume that $\langle\chi\rangle_{\Gamma}\approx\langle\chi\rangle_{\mathcal{B}}$, then $\langle c_1\rangle_{\Gamma}\approx\langle c_1\rangle_{\mathcal{B}}$ and

$$\langle c_0\rangle_{\mathcal{B}}^a + \varepsilon a\langle c_0\rangle_{\mathcal{B}}^{a-1}\langle c_1\rangle_{\Gamma} \approx \langle c_0\rangle_{\mathcal{B}}^a + \varepsilon a\langle c_0\rangle_{\mathcal{B}}^{a-1}\langle c_1\rangle_{\mathcal{B}} = \langle c\rangle_{\mathcal{B}}^a + O\left(\varepsilon^2\right). \tag{A.27}$$

The previous approximation can be derived by observing that

$$\langle c\rangle_{\mathcal{B}}^a = \left(\langle c_0\rangle_{\mathcal{B}} + \varepsilon\langle c_1\rangle_{\mathcal{B}}\right)^a + \mathcal{O}\left(\varepsilon^2\right) = \sum_{\substack{\lambda_0+\lambda_1=a \\ \lambda_1<2 \\ 0\le\lambda_i\in\mathbb{Z}}}\binom{a}{\lambda_0,\lambda_1}\varepsilon^{\lambda_1}\langle c_0\rangle_{\mathcal{B}}^{\lambda_0}\langle c_1\rangle_{\mathcal{B}}^{\lambda_1} = \langle c_0\rangle_{\mathcal{B}}^a + \varepsilon a\langle c_0\rangle_{\mathcal{B}}^{a-1}\langle c_1\rangle_{\mathcal{B}} + \mathcal{O}\left(\varepsilon^2\right). \tag{A.28}$$

Substitution of Eq. (A.27) into Eq. (A.26) leads to Eq. (21), which governs the dynamics of $\langle c\rangle_{\mathcal{B}}$ up to ε^2.

References

Auriault, J.L., Adler, P.M., 1995. Taylor dispersion in porous media: analysis by multiple scale expansions. Adv. Water Resour. 18 (4), 217–226.

Battiato, I., Tartakovsky, D.M., Tartakovsky, A.M., Scheibe, T., 2009. On breakdown of macroscopic models of mixing-controlled heterogeneous reactions in porous media. Adv. Water Resour. 32, 1664–1673.

Broyda, S., Dentz, M., Tartakovsky, D.M., 2010. Probability density functions for advective–reactive transport in radial flow. Stoch. Environ. Res. Risk Assess. doi:10.1007/s00477-010-0401-4.

Hesse, F., Radu, F.A., Thullner, M., Attinger, S., 2009. Upscaling of the advection–diffusion-reaction equation with Monod reaction. Adv. Water Resour. 32, 1336–1351.

Hornung, U., 1997. Homogenization and Porous Media. Springer, New York.
Knabner, P., Duijn, C.J.V., Hengst, S., 1995. An analysis of crystal dissolution fronts in flows through porous media. Part 1: Compatible boundary conditions. Adv. Water Resour. 18 (3), 171–185.
Knutson, C., Valocchi, A., Werth, C., 2007. Comparison of continuum and pore-scale models of nutrient biodegradation under transverse mixing conditions. Adv. Water Resour. 30 (6–7), 1421–1431.
Li, L., Peters, C., Celia, M., 2006. Upscaling geochemical reaction rates using pore-scale network modeling. Adv. Water Resour. 29, 1351–1370.
Lichtner, P.C., Tartakovsky, D.M., 2003. Upscaled effective rate constant for heterogeneous reactions. Stoch. Environ. Res. Risk Assess. 17 (6), 419–429.
Maloy, K.J., Feder, J., Boger, F., Jossang, T., 1998. Fractal structure of hydrodynamic dispersion in porous media. Phys. Rev. Lett. 61 (82), 2925.
Mikelic, A., Devigne, V., van Duijn, C., 2006. Rigorous upscaling of the reactive flow through a pore, under dominant Péclet and Damköhler numbers. SIAM J. Math. Anal. 38 (4), 1262–1287.
Morse, J.W., Arvidson, R.S., 2002. The dissolution kinetics of major sedimentary carbonate minerals. Earth Sci. Rev. 58, 51–84.
Neuman, S.P., Tartakovsky, D.M., 2009. Perspective on theories of anomalous transport in heterogeneous media. Adv. Water Resour. 32 (5), 670–680.
Nitsche, L.C., Brenner, H., 1989. Eulerian kinematics of flow through spatially periodic models of porous media. Arch. Ration. Mech. Anal. 107 (3), 225–292.
Tartakovsky, A.M., Tartakovsky, D.M., Scheibe, T.D., Meakin, P., 2008. Hybrid simulations of reaction–diffusion systems in porous media. SIAM J. Sci. Comput. 30 (6), 2799–2816.
Tartakovsky, D.M., Dentz, M., Lichtner, P.C., 2009. Probability density functions for advective–reactive transport in porous media with uncertain reaction rates. Water Resour. Res. 45, W07414.